Coral Reefs (2012) 31:1201–1213
DOI 10.1007/s00338-012-0952-6

REPORT

Microenvironmental changes support evidence of photosynthesis and calcification inhibition in *Halimeda* under ocean acidification and warming

S. Sinutok · R. Hill · M. A. Doblin · M. Kühl · P. J. Ralph

Received: 17 April 2012 / Accepted: 21 August 2012 / Published online: 8 September 2012

Abstract The effects of elevated CO_2 and temperature on photosynthesis and calcification of two important calcifying reef algae (*Halimeda macroloba* and *Halimeda cylindracea*) were investigated with O_2 microsensors and chlorophyll *a* fluorometry through a combination of two pCO_2 (400 and 1,200 μatm) and two temperature treatments (28 and 32 °C) equivalent to the present and predicted conditions during the 2100 austral summer. Combined exposure to pCO_2 and elevated temperature impaired calcification and photosynthesis in the two *Halimeda* species due to changes in the microenvironment around the algal segments and a reduction in physiological performance. There were no significant changes in controls over the 5-week experiment, but there was a 50–70 % decrease in photochemical efficiency (maximum quantum yield), a 70–80 % decrease in O_2 production and a threefold reduction in calcification rate in the elevated CO_2 and high temperature treatment. Calcification in these species is closely coupled with photosynthesis, such that a decrease in photosynthetic efficiency leads to a decrease in calcification. Although pH seems to be the main factor affecting *Halimeda* species, heat stress also has an impact on their photosystem II photochemical efficiency. There was a strong combined effect of elevated CO_2 and temperature in both species, where exposure to elevated CO_2 or temperature alone decreased photosynthesis and calcification, but exposure to both elevated CO_2 and temperature caused a greater decline in photosynthesis and calcification than in each stress individually. Our study shows that ocean acidification and ocean warming are drivers of calcification and photosynthesis inhibition in *Halimeda.* Predicted climate change scenarios for 2100 would therefore severely affect the fitness of *Halimeda*, which can result in a strongly reduced production of carbonate sediments on coral reefs under such changed climate conditions.

Keywords Chlorophyll fluorescence · Climate change · Microsensor · Macroalgae · Coral reefs

Communicated by Biology Editor Dr. Anastazia Banaszak

S. Sinutok · R. Hill (✉) · M. A. Doblin · M. Kühl · P. J. Ralph
Plant Functional Biology and Climate Change Cluster, School of the Environment, University of Technology Sydney, PO Box 123, Broadway, Sydney, NSW 2007, Australia
e-mail: ross.hill@unsw.edu.au

Present Address:
R. Hill
Centre for Marine Bio-Innovation and Sydney Institute of Marine Science, School of Biological, Earth and Environmental Sciences, The University of New South Wales, Sydney, NSW 2052, Australia

M. Kühl
Marine Biology Section, Department of Biology, University of Copenhagen, Strandpromenaden 5, 3000 Helsingør, Denmark

M. Kühl
Singapore Centre on Environmental Life Sciences Engineering, School of Biological Sciences, Nanyang Technological University, Nanyang Avenue, Singapore

Introduction

The anthropogenic use of fossil fuels, industrialization, deforestation and agricultural activities has raised the concentration of carbon dioxide (CO_2) in the atmosphere and increased CO_2 dissolution into the surface ocean (Gattuso and Lavigne 2009). This has stimulated global warming and more acidic conditions, that is, a pH decrease in the ocean's surface layer. The latter affects the inorganic carbon speciation inducing further changes in seawater

chemistry including a reduction in carbonate ion (CO_3^{2-}) abundance and a decreased aragonite saturation state (Feely et al. 2004) leading to a decrease in the capacity for marine calcifiers to produce their $CaCO_3$ skeleton (Diaz-Pulido et al. 2007; Fujita et al. 2011; Sinutok et al. 2011). Under such conditions, non-calcifying macrophytes such as seagrasses and fleshy algae may therefore have benefits over calcifying algae, as evidenced in naturally high CO_2 regions, such as the volcanic vents off Ischia Island, Italy (Hall-Spencer et al. 2008). These studies point towards likely consequences of acidification for marine ecosystems and predict an expected reduction in calcifier diversity and abundance, which will result in significant changes in habitat structure and function (Gao et al. 1993; Hall-Spencer et al. 2008; Kleypas and Yates 2009).

Halimeda is a sediment-dwelling, calcifying siphonalean green macroalga, which is widely distributed in tropical and subtropical marine environments, where it plays a major role as a carbonate sediment producer. In coral reef ecosystems, *Halimeda* is known to produce around 2.2 kg of $CaCO_3$ m^{-2} $year^{-1}$, which is equivalent to the rate of production by scleractinian corals (Smith and Kinsey 1976; Drew 1983). *Halimeda* thus provides essential ecological services as a habitat-forming bioengineer in these marine ecosystems (Drew 1983). The algal thallus consists of articulated, plate-like and calcified segments, which are joined together by small, uncalcified nodes forming branching chains (Blaxter et al. 1980). *Halimeda* precipitates $CaCO_3$ in the form of aragonite into the intercellular (utricular) space of its segments (Borowitzka et al. 1974; Borowitzka and Larkum 1977). New segments can be formed rapidly, involving a complex sequence of local decalcification, filament extension and chloroplast migration from old segments overnight, followed by the onset of calcification (Larkum et al. 2011).

The current saturation state of aragonite, Ω_a, is 3.5–4.0 for the Pacific region and is expected to decline ~30 % by 2,050 under predicted future climate scenarios (Kleypas et al. 1999; Guinotte et al. 2003). Elevated pCO_2 has previously been shown to reduce calcification, growth and productivity in the articulate coralline alga *Corallina pilulifera* and *C. officinalis* and crustose coralline algae (Kuffner et al. 2007; Anthony et al. 2008; Hofmann et al. 2012). Combined effects of elevated temperature and pCO_2 cause bleaching, calcium carbonate dissolution and erosion in the reef-building corals *Acropora intermedia* and *Porites lobata* (Anthony et al. 2008). Recently, Sinutok et al. (2011) showed that pCO_2 levels representative of modelled climate scenarios for the years 2100 and 2200 (Houghton 2009) significantly reduced calcification and photosynthetic efficiency in *Halimeda*. Such impairment was attributed to lower seawater pH and reduced abundance of CO_3^{2-} as already shown by Borowitzka and Larkum (1976b), leading to a decline in calcification rate, calcium carbonate crystal size, photosynthetic pigment content (chlorophyll *a* and *b*) and photosynthetic efficiency. The decline of photosynthesis and calcification was amplified by concurrent exposure to elevated temperatures, that is, 2–6 °C above typical summer average seawater temperature. While bulk seawater characteristics had an obvious impact on photosynthesis and calcification, the microenvironmental conditions and regulatory mechanisms involved in such impairment of photosynthesis and calcification in *Halimeda* under elevated pCO_2 and temperature remain unknown.

Microsensors enable mapping of physicochemical microenvironment of marine calcifying organisms at high spatio-temporal resolution (De Beer and Larkum 2001; Al-Horani 2005; Köhler-Rink and Kühl 2005). Oxygen (O_2), carbon dioxide (CO_2), pH and calcium (Ca^{2+}) microsensors have been used to study the photosynthesis and calcification in *Halimeda discoidea*. De Beer and Larkum (2001) showed that calcium dynamics and calcification in *H. discoidea* are determined by the pH at the segment surface, and they hypothesized that acidification of sea water would decrease the calcification rate. Here, we investigate the effects of ocean acidification and ocean warming on the microenvironment and photosynthesis of *Halimeda* spp. using O_2 microsensors and chlorophyll *a* fluorometry and present the first data on how the microenvironment, photosynthesis and respiration of *Halimeda* are affected by changing pCO_2 and temperature conditions.

Materials and methods

Sample collection and experimental design

Halimeda macroloba and *H. cylindracea* specimens (thallus length of 13–20 cm) were collected by hand from Heron Island reef flat (Southern Great Barrier Reef, Australia; 151°55′E, 23°27′S) at low tide at 0.3 m depth and maintained at the University of Technology, Sydney, for 2 months in a 500-L aquarium with artificial seawater (26 °C, pH 8.1, salinity of 33) under an incident irradiance (PAR, 400–700 nm) of 250 μmol photons m^{-2} s^{-1} over a 12-h/12-h light–dark cycle. Seawater concentrations of carbonate, calcium, nitrate and phosphate were maintained at 2.3, 10, <0.0016 and 0.0005 mM, respectively. Whole specimens of *Halimeda* were randomly allocated to one of four treatments (1 sample per tank, 4 tanks per treatment): (1) control (pH 8.1 and 28 °C; equivalent to current summer temperature average at Heron Island and a pCO_2 of 400 μatm), (2) elevated temperature only (pH 8.1 and 32 °C), (3) reduced pH only (pH 7.7 and 28 °C) and (4) a combination of both low pH and high temperature (pH 7.7 and 32 °C). The elevated temperature and decreased pH

Table 1 Parameters of the carbonate system; total alkalinity (TA), CO_2 partial pressure (pCO_2), dissolved inorganic carbon species (DIC; CO_2, CO_3^{-2}, HCO_3^-), total DIC and saturation state of sea water with respect to aragonite (Ω_a) from each pH (8.1, 7.7) and temperature (28, 32 °C) treatment used in this study

Treatment		TA (mmol kg^{-1})	pCO_2 (µatm)	CO_2 (mmol kg^{-1})	CO_3^{-2} (mmol kg^{-1})	HCO_3^- (mmol kg^{-1})	DIC (mmol kg^{-1})	Ω_a
pH	Temp (°C)							
8.1	28	2.327 ± 0.002	380.8 ± 0.4	0.010 ± 0.001	0.239 ± 0.024	1.745 ± 0.020	1.993 ± 0.020	3.87 ± 0.01
8.1	32	2.326 ± 0.036	444.9 ± 7.4	0.010 ± 0.002	0.239 ± 0.039	1.742 ± 0.030	1.881 ± 0.033	3.97 ± 0.07
7.7	28	2.512 ± 0.030	1208.1 ± 14.6	0.032 ± 0.004	0.122 ± 0.015	2.219 ± 0.027	2.373 ± 0.028	1.97 ± 0.02
7.7	32	2.508 ± 0.015	1394.2 ± 8.6	0.034 ± 0.002	0.123 ± 0.007	2.212 ± 0.014	2.369 ± 0.014	2.05 ± 0.01

Data represent means ($n = 3$, ±SE)

treatments represent conditions predicted by current climate change models for the year 2100, equivalent to a 4 °C temperature rise and a pCO_2 concentration of 1200 µatm (Houghton 2009). Samples were ramped from 26 °C and a pH of 8.1 to their treatment conditions over 1 week and were maintained for another 4 weeks in their treatments. pCO_2 and temperature were controlled using pH controllers (7020/2, Tunze, Germany) connected to CO_2 bubblers, and water thermostats (TC10, Teco, Italy), as described in Sinutok et al. (2011). Salinity was set at 33, and quantum irradiance (PAR) at the sample surface was 300 µmol photons m^{-2} s^{-1} on a 12/12-h light–dark cycle (light on at 0900 h and light off at 2100 h). The water quality was maintained identical to the holding tank with carbonate, calcium, nitrate and phosphate concentrations of 2.3, 10, <0.0016 and 0.0005 mM, respectively. Total alkalinity (TA) was measured weekly by titrating 30 g of sea water with 0.1 M HCl in an autotitrator (DL50, Mettler Toledo). The speciation of dissolved inorganic carbon (DIC) into CO_2, CO_3^{-2} and HCO_3^-, the CO_2 partial pressure (pCO_2) and the saturation state of sea water with respect to aragonite (Ω_a) were determined using CO2SYS (version 01.05; Brookhaven National Laboratory; Lewis and Wallace 1998). A summary of the TA, total inorganic carbon (DIC), DIC speciation, pCO_2 and Ω_a from each temperature (28 °C, 32 °C) and pH (8.1, 7.7) treatment is shown in Table 1.

Calcification

Whole specimen calcification rates were determined using the buoyant weight technique (Jokiel et al. 2008; Sinutok et al. 2011) with weight comparisons made between measurements at the start and end of the experimental period. The buoyant weight technique is a reliable measure of calcification by weighing each sample in sea water of known density and applying Archimedes' principle to compute the dry weight of the sample in the air (Jokiel et al. 1978; Langdon et al. 2010). Samples were placed on a glass Petri dish hung below an electronic balance (AB204-S, Mettler Toledo, USA; accuracy ~0.1 mg) using nylon thread suspended in sea water.

Variable chlorophyll *a* fluorescence

Photosynthetic performance of *Halimeda* was quantified every 10 days over the duration of the experiment by variable chlorophyll fluorescence measurements using a 6-mm-diameter fibre-optic probe connected to a Diving-PAM fluorometer (Walz, Germany). Photosystem II (PSII) photochemical efficiency was measured as the maximum quantum yield of PSII (F_V/F_M) at 0900 h (before lights were turned on) and the effective quantum yield ($\Delta F/F_M'$) at 1300 h, after which the maximum excitation pressure over photosystem II (Q_m) was calculated. The parameter Q_m quantifies non-photochemical quenching and is defined as $Q_m = 1-(\Delta F/F_M')/(F_V/F_M)$ according to Iglesias-Prieto et al. (2004).

Photosynthetic pigment concentration

Concentrations of chlorophyll (Chl) *a* and *b* were determined in extracts of *Halimeda* samples using the spectrophotometric method of Ritchie (2008) at the beginning and end of the 5-week experiment and expressed in µg Chl g^{-1} fresh weight (fw) of *Halimeda*. Chl *a* and *b* were extracted by grinding samples in 4 ml of 90 % acetone at 4 °C followed by extraction in darkness for 24 h. Subsequently, samples were centrifuged at 1,500*g* for 10 min, after which the supernatant was transferred to a quartz cuvette and its absorbance measured at 647 and 664 nm on a spectrophotometer (Cary 50, Varian, Australia).

Oxygen microsensors

Microsensor measurements of O_2 concentration were performed in a 2-L flow chamber as described by Köhler-Rink and Kühl (2000) at the start of the experiment, and after 3 and 5 weeks. Segments of *H. macroloba* (0.8–1.2 cm long)

and *H. cylindracea* (1.5–2.0 cm long) from the treatment tanks were placed on the bottom of the chamber, with a water flow of 2.5 cm s^{-1} maintained by a submersible aquarium pump. The thallus surface O_2 concentration and rate of O_2 production was determined under quantum irradiances of 0, 80, 150, 230, 570 and 900 µmol photons m^{-2} s^{-1}, as controlled by a fibre-optic halogen lamp (KL-2500, Schott, Germany) equipped with a collimating lens and a heat filter. The O_2 microsensor was mounted on a motorized micromanipulator (Oriel Encoder Mike, United States) which, along with data acquisition, was regulated by Profix software (Pyro-Science, Denmark).

Oxygen concentration profiles and the rate of gross photosynthetic O_2 production were measured at the surface (0–300 µm) of *H. macroloba* and *H. cylindracea* using an O_2 microelectrode (OX-100, Unisense, Denmark) connected to a picoammeter (PA2000, Unisense, Denmark) and a strip chart recorder (BD12E, Kipp&Zonen, the Netherlands). The microelectrode had an outer tip diameter of 100 µm, a 90 % response time of <8 s and a stirring sensitivity of <1.5 %. A linear calibration of the microelectrode was performed at chamber temperature in air-saturated sea water and O_2-free sea water (made anoxic by addition of sodium dithionite). A proxy for gross photosynthesis (P_y; nmol O_2 cm^{-3} s^{-1}) at the specimen surface of *Halimeda* spp. was estimated after a short experimental light–dark shift by measuring the rate of O_2 depletion over the first 10 s after darkening (Revsbech et al. 1981; Köhler-Rink and Kühl 2000). According to the limitation of microsensor response time (<8 s), the gross photosynthesis from this measurement is underestimated and represents an integral over a large sample volume; however, it can still be used to compare between treatments.

The local diffusive O_2 flux (J; nmol O_2 cm^{-2} s^{-1}), that is, the O_2 uptake rate in darkness and the net O_2 production rate in light, was calculated from measured steady-state O_2 concentration profiles by Fick's first law (Köhler-Rink and Kühl 2000): $J = -D_0\ (dC/dz)$ where D_0 is the molecular diffusion coefficient in sea water at experimental salinity and temperature, and dC/dz is the linear slope of the O_2 concentration profile in the diffusive boundary layer (DBL) above the *Halimeda* thallus surface. We note that the presence of microsensor above the *Halimeda* thallus can compress the diffusive boundary layer leading to a locally accelerated flow around the microsensor tip (Glud et al. 1995). However, as flow conditions were identical between treatments, diffusive fluxes can still be compared.

Statistical analysis

To identify significant differences ($\alpha = 0.05$) among treatments in calcification, Chl *a* and *b* concentration, a series of one-way and two-way analysis of variance (ANOVA) tests were performed (SPSS v17). To determine significant differences among treatments and over time in chlorophyll fluorescence parameters (F_V/F_M, $\Delta F/F_M'$, Q_m), O_2 concentration at the thallus surface, diffusive O_2 flux and proxy gross photosynthesis, repeated measures analysis of variance (rmANOVA) tests, with pH and temperature as between-subject independent variables and time as a within-subject independent variable (repeated measures factor), were performed. Tukey's honestly significant difference post hoc tests were used to identify statistically distinct groups. If data did not meet the assumptions of normality (Kolmogorov–Smirnov test) and equal variance (Levene's test), the data were transformed using $\log_{10}$ or square root.

Table 2 Calcification rate (% increase day^{-1}) and chlorophyll (Chl) *a* and *b* concentration (µg g^{-1} fw) of *H. macroloba* and *H. cylindracea* after 5 weeks in each pH and temperature treatment

	Calcification rate (% per day)	Chl *a* (µg g^{-1} fw)	Chl *b* (µg g^{-1} fw)
H. macroloba			
Time 0	–	42.1 ± 5.8	24.5 ± 3.0
pH 8.1, 28 °C	0.45 ± 0.07	45.8 ± 5.1	32.5 ± 3.8
pH 8.1, 32 °C	0.26 ± 0.14	39.4 ± 3.6	24.5 ± 2.7
pH 7.7, 28 °C	−0.51 ± 0.16	28.5 ± 2.1	18.2 ± 2.5
pH 7.7, 32 °C	−1.57 ± 0.71	29.7 ± 2.5	20.8 ± 3.6
P value			
pH	0.003*	0.005*	0.012*
Temperature	0.123	0.529	0.412
pH*Temperature	0.269	0.374	0.115
H. cylindracea			
Time 0	–	43.6 ± 3.3	28.9 ± 1.7
pH 8.1, 28 °C	0.38 ± 0.14	43.3 ± 2.5	24.1 ± 2.3
pH 8.1, 32 °C	0.26 ± 0.18	34.5 ± 1.3	21.3 ± 2.1
pH 7.7, 28 °C	−0.29 ± 0.08	29.4 ± 1.2	17.3 ± 2.7
pH 7.7, 32 °C	−0.31 ± 0.04	26.2 ± 0.7	16.0 ± 1.9
P value			
pH	<0.001*	<0.001*	0.014*
Temperature	0.586	0.011*	0.375
pH*Temperature	0.697	0.189	0.732

Data represent means ($n = 4$, mean ± SE)

* Signifies $p < 0.05$

Results

Calcification rate

The calcification rates of *H. macroloba* and *H. cylindracea* were slightly positive in the control (pH 8.1, 28 °C; <0.5 % increase per day; Table 2) and the elevated

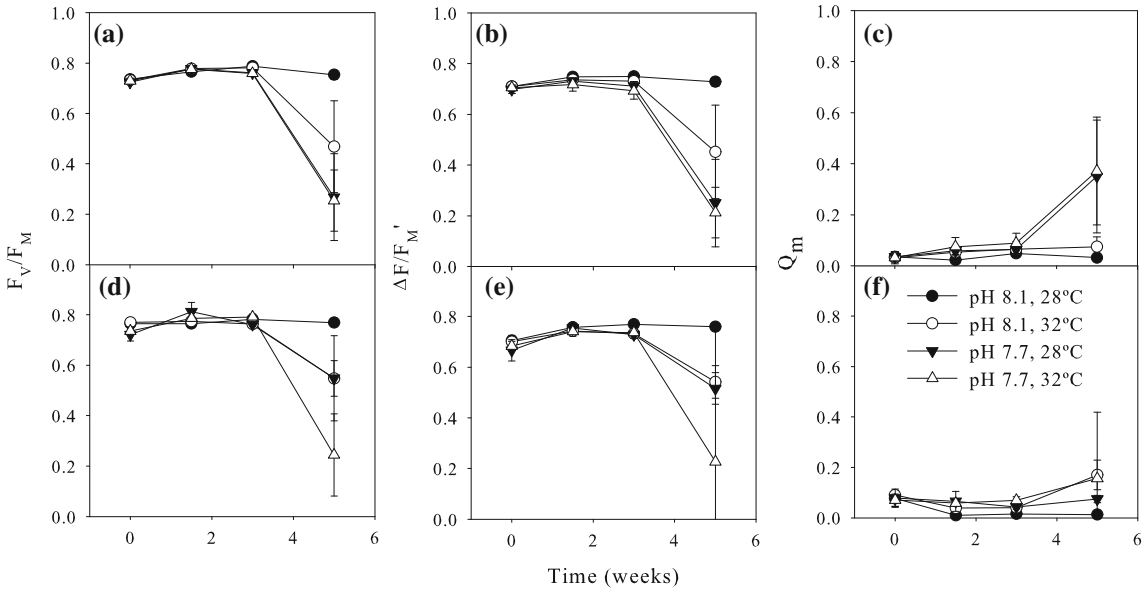

Fig. 1 Maximum quantum yield (F_V/F_M), effective quantum yield ($\Delta F/F_M'$) and maximum excitation pressure over photosystem II (Q_m) of **a–c** *H. macroloba* and **d–f** *H. cylindracea* in each pH and temperature treatment over the length of the experimental period. Data represent means ($n = 4$, ±SE)

temperature treatment (pH 8.1, 32 °C; <0.3 % per day), but were negative in the elevated pCO_2 treatments both at control and elevated temperature (pH 7.7, 28 °C and pH 7.7, 32 °C; −0.2 to −1.6 % per day; Table 2). *H. macroloba* and *H. cylindracea* had significantly lower calcification in the reduced pH treatments at both 28 and 32 °C than in the control treatment ($p = 0.003$ and $p < 0.001$, respectively; Table 2). The calcification rate of *H. macroloba* in the elevated CO_2 and elevated temperature treatment was not significantly different from calcification in *H. cylindracea* in the same treatment ($p > 0.05$).

Photosynthetic pigment concentration

Initial Chl *a* and *b* concentrations were 42.1 ± 5.8 and 24.5 ± 3.0 μg g^{-1} (mean ± SE) in *H. macroloba* and 43.6 ± 3.3 and 28.9 ± 1.7 μg g^{-1} (mean ± SE) in *H. cylindracea*, respectively (Table 2). After 5 weeks, there were no significant changes in Chl *a* and *b* concentration in *H. macroloba* in the control (pH 8.1, 28 °C; $p = 0.651$ for Chl *a*; $p = 0.151$ for Chl *b*) and elevated temperature treatments (pH 8.1, 32 °C; $p = 0.788$ for Chl *a*; $p = 0.997$ for Chl *b*) or in the control treatment for *H. cylindracea* (pH 8.1, 28 °C; $p = 0.946$ for Chl *a*; $p = 0.146$ for Chl *b*). In *H. cylindracea* at pH 8.1, 32 °C, Chl *a* concentration significantly declined to 34.5 ± 1.3 μg g^{-1} (mean ± SE; $p < 0.046$), whereas there were no significant changes in Chl *b* concentration ($p > 0.05$; Table 2). The Chl *a* and *b* concentration in *H. macroloba* and *H. cylindracea* significantly declined at pH 7.7 within the 28 and 32 °C treatment ($p < 0.05$; Table 2).

Variable chlorophyll fluorescence

The maximum quantum yield (F_V/F_M), effective quantum yield ($\Delta F/F_M'$) and maximum excitation pressure on PSII (Q_m) in the control treatment remained constant over the experimental period in both species of *Halimeda*, ranging from 0.73–0.79, 0.70–0.77 and 0.01–0.08, respectively ($p > 0.05$; Fig. 1a, d). There was, however, a significant decrease (50–70 %) in F_V/F_M and $\Delta F/F_M'$ in *H. macroloba* and *H. cylindracea* at week 5 under elevated CO_2 and temperature treatments (pH 8.1, 32 °C, pH 7.7, 28 °C and pH 7.7, 32 °C; $p < 0.001$; Fig. 1a–b, d–e). Both *Halimeda* species under elevated CO_2 and temperature showed very large Q_m values (0.2–0.6) at week 5. At this time, *H. macroloba* exhibited significantly higher Q_m values under elevated CO_2 in both temperature treatments ($p < 0.022$; Fig. 1c), whereas *H. cylindracea* showed significantly higher Q_m values in all treatments except the control ($p < 0.038$; Fig. 1f).

O_2 microenvironment

Oxygen concentration profiles measured towards the thallus surface of *H. macroloba* and *H. cylindracea* were affected by irradiance, pCO_2, temperature and time of exposure to elevated pCO_2 and temperature ($p < 0.05$; Figs. 2, 3, 4). Initially, in all light treatments, the O_2 concentration surpassed the ambient O_2 concentration in the surrounding water (209 μM) at the upper boundary of the diffusive boundary layer ~150 μm above the *H. macroloba* segment surface and reached an O_2 concentration of

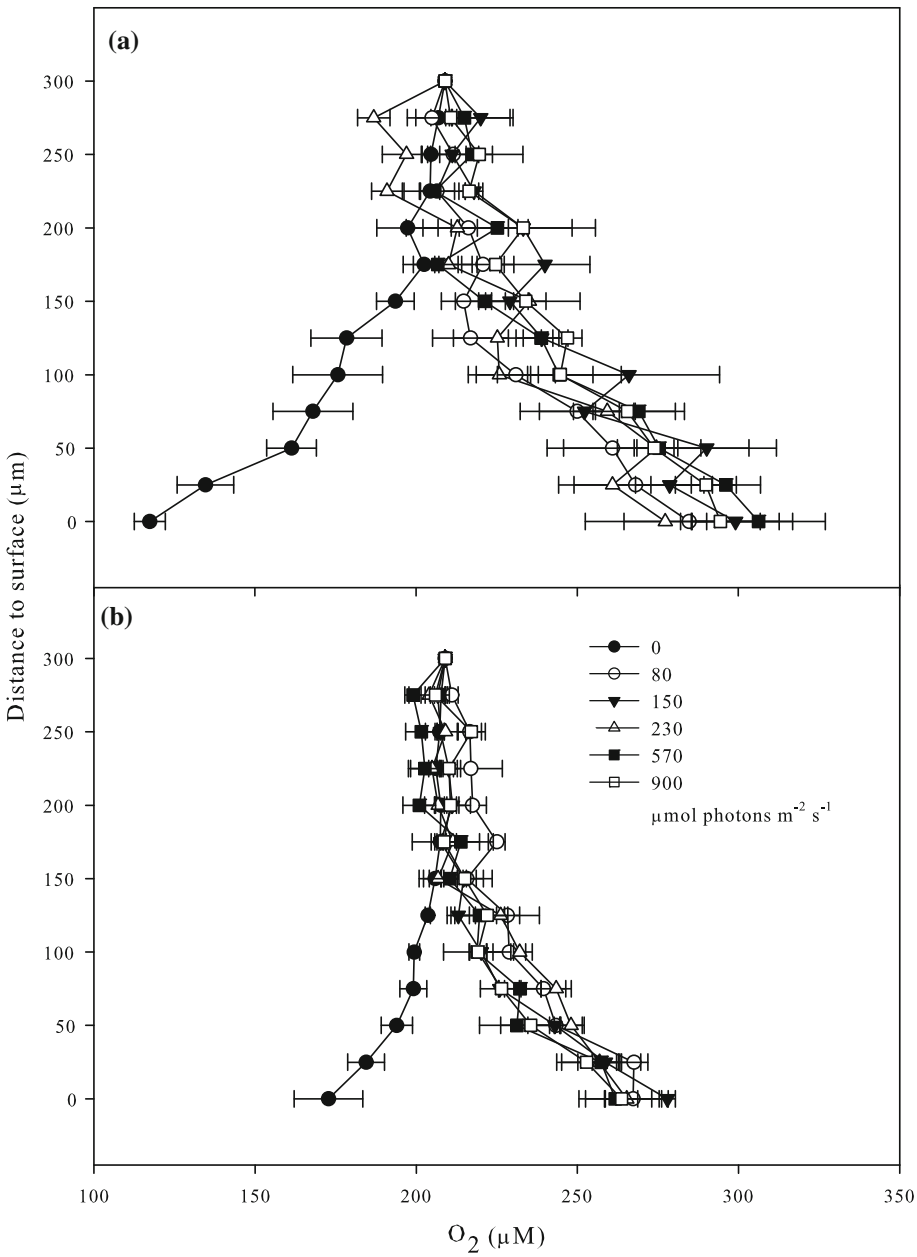

Fig. 2 Oxygen concentration profile towards the thallus surface measured at week 1 from **a** *H. macroloba* and **b** *H. cylindracea* at each experimental irradiance (0, 80, 150, 230, 570 and 900 µmol photons m^{-2} s^{-1}). Data represent means ($n = 4$, ±SE)

277–306 µM at the segment surface (Fig. 2a). In the dark, the ambient O_2 concentration decreased from 209 µM at 150 µm above the *H. macroloba* segment to 117 µM at the segment surface (Fig. 2a). The O_2 concentration at the segment surface in all light treatments was higher compared to when in darkness ($p < 0.001$; Fig. 2a).

After 3 and 5 weeks, the O_2 concentration profiles in *H. macroloba* showed different responses in each pH and temperature treatment (Fig. 3a–h). The O_2 concentration at the shell surface changed over time and between pH and temperature treatments ($p < 0.001$; Figs. 2a, 3a–h). After 3 weeks, the control treatment of *H. macroloba* showed an increasing O_2 concentration at the segment surface reaching ~230–330 µM in all light treatments and a decrease in O_2 concentration to 202 µM under dark conditions (Fig. 3a). Significant increases in segment surface O_2 concentration were found in the pH 8.1, 32 °C treatment reaching 333–461 µM at all irradiance levels ($p < 0.001$), whereas segment surface O_2 concentration significantly decreased to 180 µM in the dark ($p < 0.001$; Fig. 3b). There was a significant decrease in segment surface O_2 concentration in the pH 7.7, 28 °C treatment at 570 and 900 µmol photons m^{-2} s^{-1} ($p < 0.001$; Fig. 3c), whereas it was not observed in *H. cylindracea*. After 5 weeks, the pH 8.1, 32 °C treatment in *H. macroloba* showed no significant changes in O_2 concentration at the segment surface ($p > 0.05$; Fig. 3f). Similar

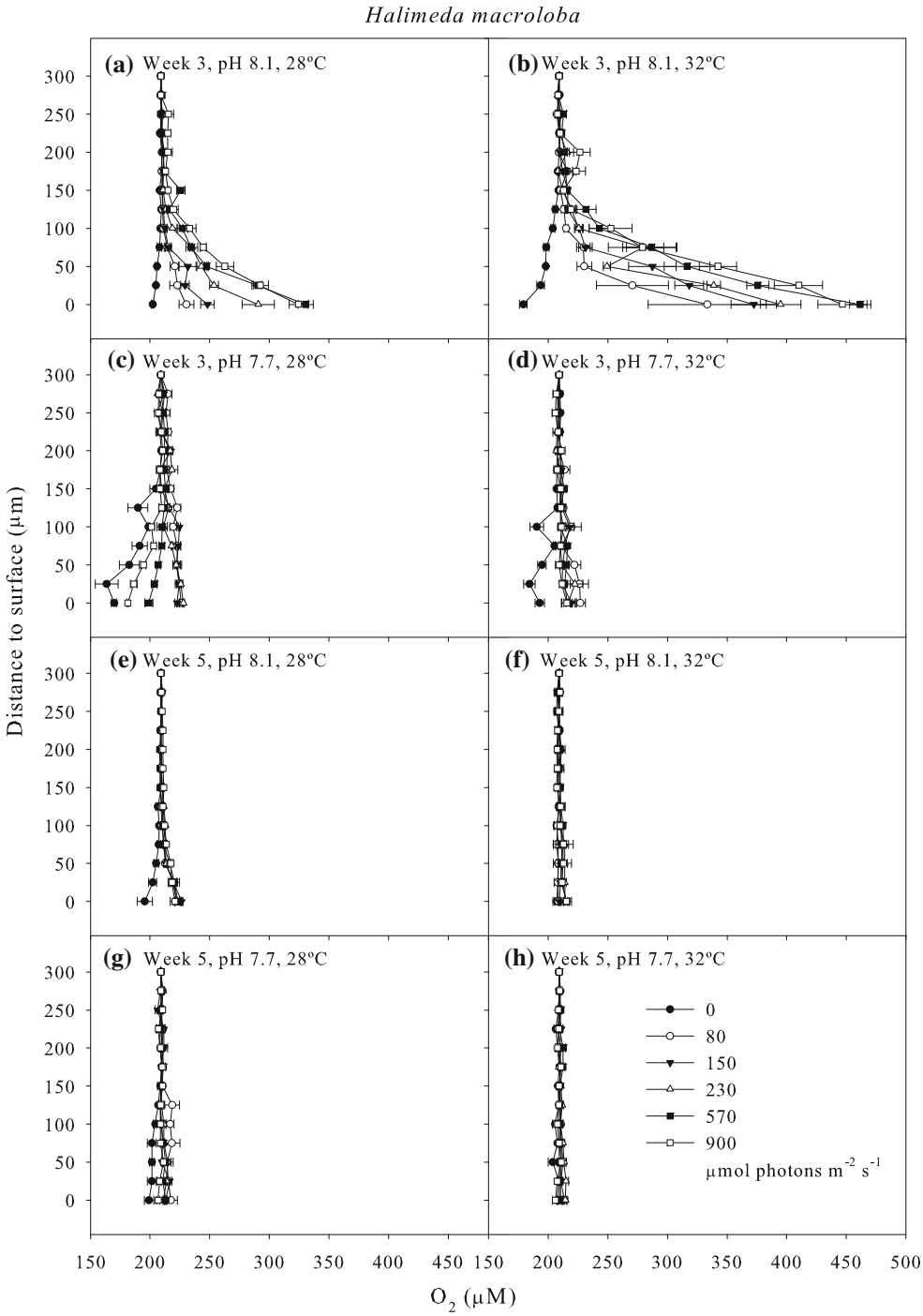

Fig. 3 Oxygen concentration profile towards the thallus surface measured at **a–d** week 3 and **e–h** week 5 from *H. macroloba* at each pH and temperature treatment at each experimental irradiance (0, 80, 150, 230, 570 and 900 µmol photons m^{-2} s^{-1}). Data represent means ($n = 4$, ± SE)

observations were seen at pH 7.7 and both temperature treatments at 3 and 5 weeks in *H. macroloba* (Fig. 3c–d, g–h).

In *H. cylindracea* at the start of the experiment, the ambient O_2 concentration increased from 209 µM at 125 µm above the segment to 260–277 µM at the segment surface when in light. A decrease to 172 µM was found at the tissue surface when in darkness (Fig. 2b). There were significant changes in O_2 concentration at the shell surface over time and between pH and temperature treatments ($p < 0.001$; Figs. 2b, 4a–h). At 3 weeks, *H. cylindracea* in the control treatment and pH 8.1, 32 °C treatment, a significant increase in O_2 concentration was found when reaching the segment surface at about 265–580 and 336–400 µM, respectively, in all light treatments ($p < 0.001$; Fig. 4a, b). In addition, a significant decrease in O_2 concentration was found when reaching the segment surface at about 128 and 184 µM in darkness, respectively ($p < 0.001$; Fig. 4a, b). No significant changes in O_2 concentration at the segment surface were observed at 3 and 5 weeks at pH 7.7 in both temperature treatments and at 5 weeks in the pH 8.1, 32 °C treatment ($p > 0.05$; Fig. 4c–d, f–h).

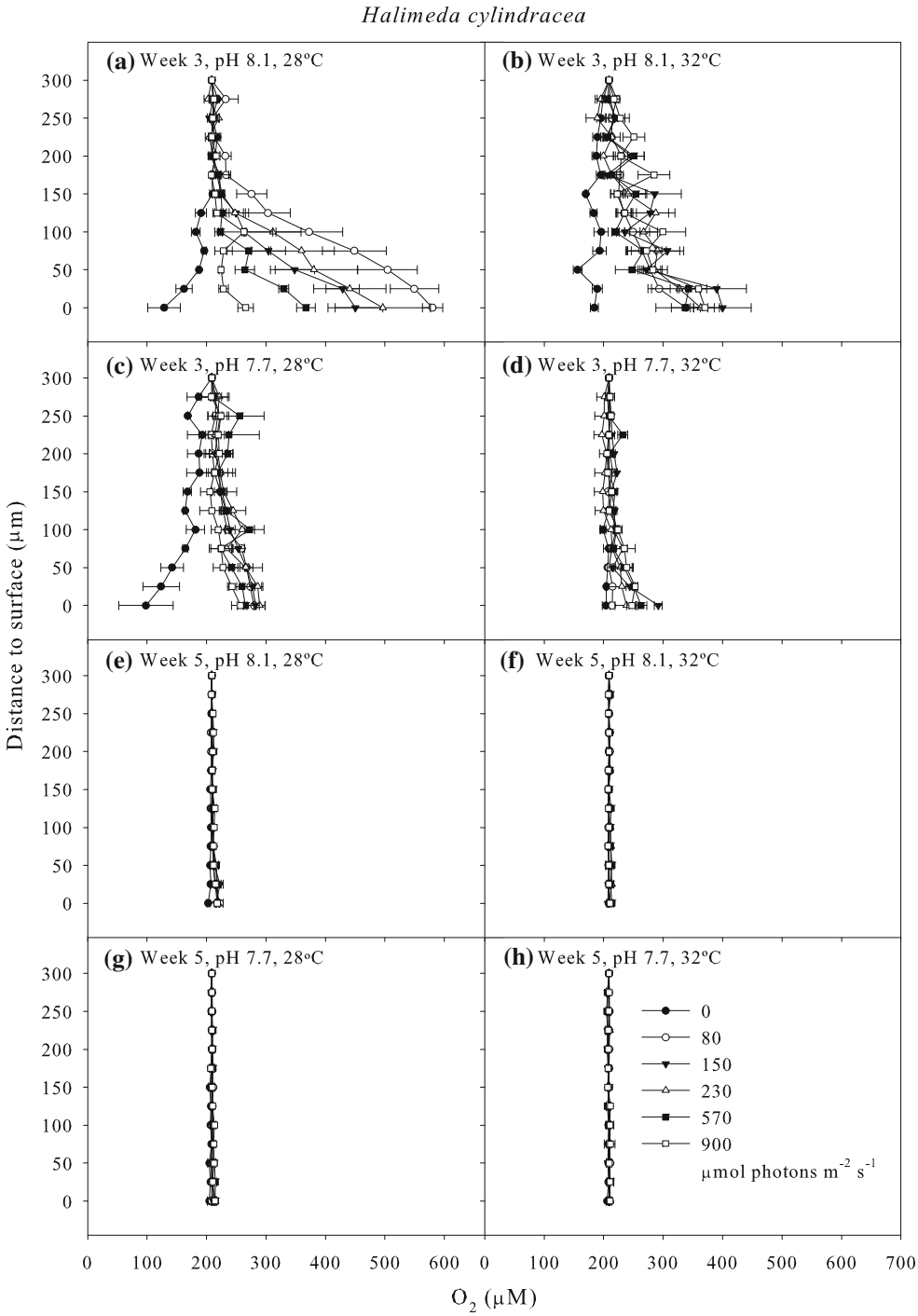

Fig. 4 Oxygen concentration profile towards the thallus surface measured at **a–d** week 3 and **e–h** week 5 from *H. cylindracea* at each experimental pH and temperature treatment at each irradiance (0, 80, 150, 230, 570 and 900 µmol photons m^{-2} s^{-1}). Data represent means ($n = 4$, ±SE)

Gross photosynthesis and O_2 flux

Estimated rates of gross photosynthesis and O_2 flux, that is, net photosynthesis, of both *Halimeda* species were influenced by CO_2 and time of exposure to elevated CO_2 and temperature ($p < 0.001$; Figs. 5, 6). In *H. macroloba*, gross photosynthesis decreased with elevated pCO_2 (pH 7.7 at both temperatures; $p < 0.001$; Fig. 5a) and long-term exposure (5 weeks) to elevated pCO_2 and temperature ($p < 0.001$; Fig. 5b). Gross photosynthesis in *H. cylindracea* also declined at week 5 at pH 7.7 at 28 and 32 °C ($p < 0.001$; Fig. 5d).

After 3 weeks, a significant decrease in the rate of O_2 efflux in light was observed in both species under elevated CO_2 conditions (pH 7.7, at both temperatures; $p < 0.001$; Fig. 6a, c). After 5 weeks, the rate of O_2 efflux in both species decreased under elevated CO_2 treatments (pH 7.7, at both temperatures for 70–80 %) ($p < 0.001$; Fig. 6b, d).

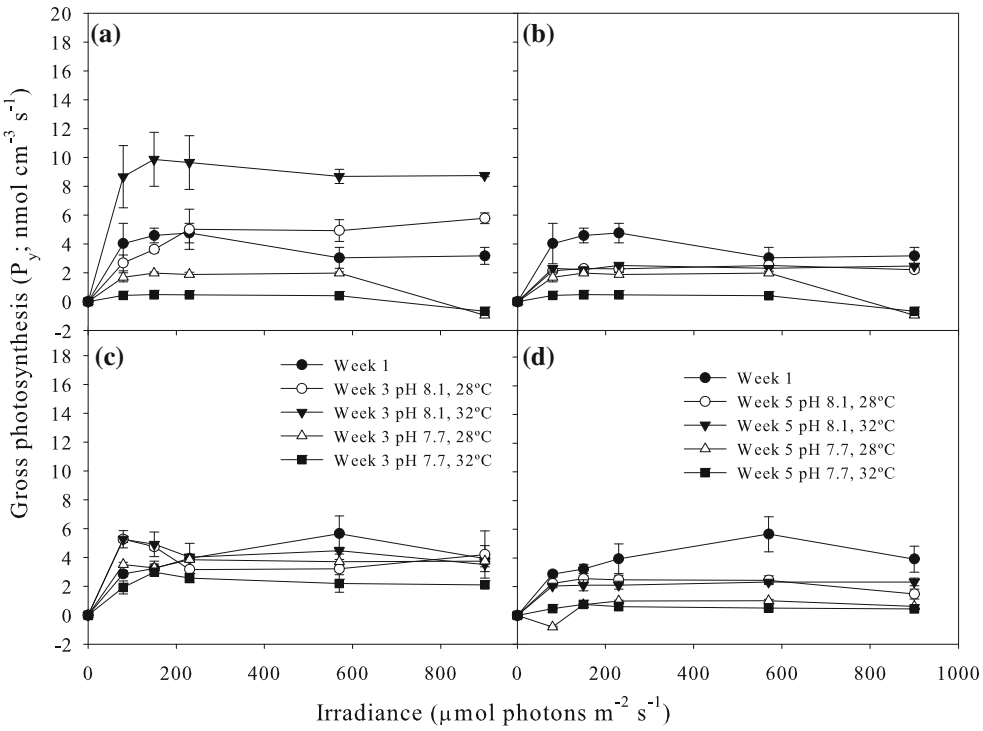

Fig. 5 Gross photosynthesis estimates (P_y; nmol O_2 cm^{-3} s^{-1}) at the thallus surface measured at week 1, 3 and 5 from **a**, **b** *H. macroloba* and **c**, **d** *H. cylindracea* in each pH and temperature treatment. Data represent means ($n = 4$, ±SE)

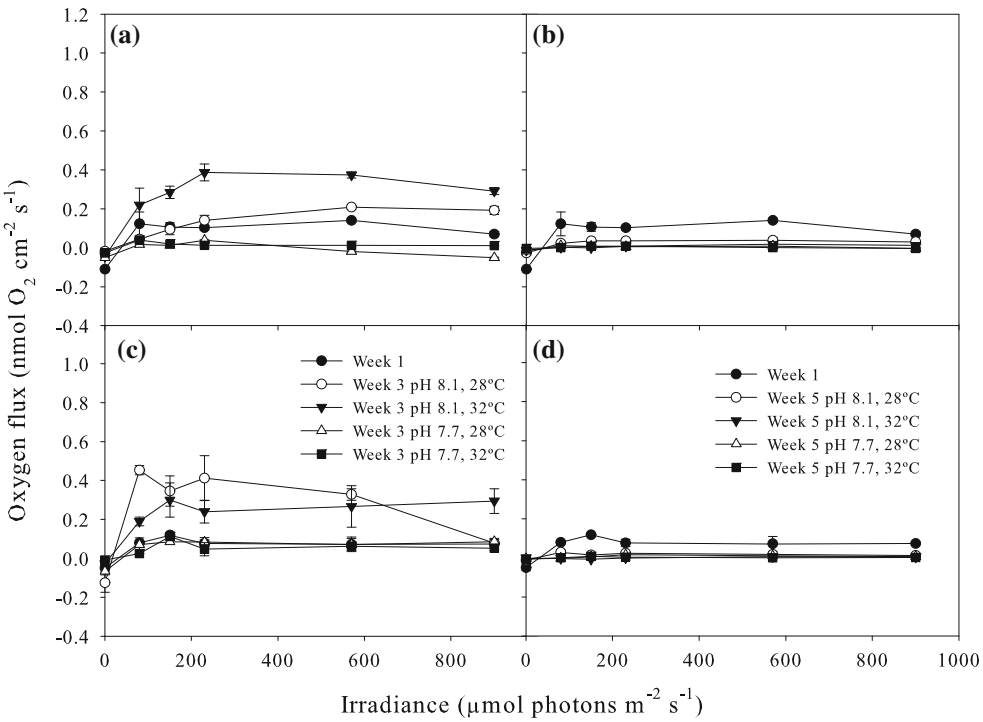

Fig. 6 Diffusive O_2 flux (nmol O_2 cm^{-2} s^{-1}) at the thallus surface measured at week 1, 3 and 5 from **a**, **b** *H. macroloba* and **c**, **d** *H. cylindracea* in each pH and temperature treatment. Data represent means ($n = 4$, ±SE)

Discussion

Previous applications of pH and O_2 microsensors have demonstrated their ability to resolve the dynamic microenvironment of calcifying reef algae, corals and foraminifera at high spatio-temporal resolution (e.g. De Beer and Larkum 2001; Al-Horani 2005; Köhler-Rink and Kühl 2005), but this is the first study to investigate the

combined effects of elevated temperature and pCO_2 on the O_2 microenvironment of *Halimeda*. Our results showed strong effects of elevated temperature and pCO_2 on the microenvironment around the segments of two *Halimeda* species, as well as strong reductions in physiological performance.

Temporal changes in productivity in response to ocean acidification and ocean warming

There was net O_2 production in the light in the control treatment over the 5-week experiment, which was reversed in darkness due to respiration. Short-term exposure (3 weeks) to elevated temperature (32 °C) and current pCO_2 (400 µatm) increased the productivity of both species, with increasing O_2 concentration and O_2 flux at the segment surface and increasing gross photosynthesis, while long-term exposure (5 weeks) to elevated temperature led to a decrease in the productivity of both species. These observations are consistent with a previous study, where high O_2 production was found after short-term (18 days) exposure to elevated temperature, while long-term exposure (35 days) resulted in decreased productivity and metabolism in these species (Sinutok et al. 2011). Although short-term exposure to elevated temperature (32 °C) may lead to increasing productivity and metabolism in this species, 32 °C was found to be an upper limit for survival (Sinutok et al. 2011). Exposure to 32 °C for 5 weeks may damage PSII, possibly by damaging the D1 protein and disrupting the thylakoid membrane stability (Warner et al. 1999; Hill et al. 2004; Allakhverdiev et al. 2008). This suggests that the potential for acclimation to thermal stress is limited. After 3 and 5 weeks under elevated CO_2 and temperature, the rate of O_2 consumption in darkness and net O_2 production in light decreased even further. This suggests that ocean acidification compounds the reduction in photosynthetic activity and elevated photoinhibition under temperature stress.

Net O_2 production and consumption in *H. macroloba* and *H. cylindracea* controls were significantly greater than in other treatments. However, we found a sharp decrease in net O_2 production in both species in controls at week 5 compared to week 1 and week 3, suggesting that the algae were relatively unhealthy. However, the photosynthetic efficiency (F_V/F_M) in the controls at week 5 did not show the same trend. This may be explained due to O_2 production measurements detecting oxygen evolved during photosynthesis which includes respiration. In contrast, F_V/F_M is a measurement of PSII photochemistry and represents the maximum efficiency at which light absorbed by PSII is used for photochemistry and indicates stress or damage in PSII (Maxwell and Johnson 2000; Schreiber 2004; Baker 2008).

Ocean acidification is more influential than ocean warming in reducing *Halimeda* productivity

Although CO_2 uptake during photosynthesis mainly occurs at the cell wall surface facing into the intercellular space (Borowitzka and Larkum 1976b), De Beer and Larkum (2001) observed that photosynthetic CO_2 uptake in *Halimeda* leads to an increase in extracellular pH at the thallus surface, whereas CO_2 and H^+ production from respiration and calcification leads to a decrease in pH. This study showed that elevated CO_2 conditions, and thus increased availability for carbon uptake, did not lead to increased O_2 production in these *Halimeda* species, suggesting that pH may be the main factor inhibiting their metabolism. A reduction in pH may disrupt the CO_2 accumulation pathway at the site of Rubisco or disrupt electron transport via the thylakoid proton gradients (Anthony et al. 2008). A reduction in photosynthesis due to these stressors will consequently have an impact on calcification due to the loss of elevated intracellular pH at the site of calcification.

Calcification is promoted under high pH conditions, as the speciation of dissolved inorganic carbon is favoured towards carbonate (Table 1), which was clearly shown in Borowitzka and Larkum (1976b). Therefore, any alterations of intracellular pH will influence calcification rate. Reduced pH as a direct consequence of ocean acidification as well as through the inhibition of photosynthesis is therefore likely to slow the rate of calcification (Borowitzka and Larkum 1976b; De Beer and Larkum 2001). Rising CO_2 will inhibit calcification by decreasing the availability of CO_3^{2-} ions required for calcium carbonate precipitation (De Beer and Larkum 2001; Feely et al. 2004; Ries 2011). Although elevated temperature leads to an increase in aragonite saturation state (less solubility of $CaCO_3$; Weyl 1959) as shown in Table 1, this increase in saturation state is not large enough to offset the pH effects, so pH seems to be the main factor affecting calcification in *Halimeda*.

Intracellular mechanisms of calcification and the interaction with respiration and production

In this study, we observed that calcification rates declined with decreasing pH, with a concomitant decline in photosynthetic efficiency. This suggests that calcification in these *Halimeda* species is closely coupled to photosynthesis, such that a decrease in photosynthetic efficiency leads to a decrease in calcification. It has been proposed that calcification and photosynthesis are tightly coupled, with calcification promoting photosynthesis by providing a proton source through calcium carbonate deposition, and these protons promote the conversion of HCO_3^- to CO_2, which is used in the dark reactions of photosynthesis

(Borowitzka 1977, 1989; McConnaughey 1989; McConnaughey and Whelan 1997). As a result, the pH in the DBL surrounding *Halimeda* increases due to CO_2 uptake for photosynthesis in the light, whereas pH decreases due to CO_2 and H^+ released from respiration and calcification (Borowitzka 1986; De Beer and Larkum 2001). pH and light also influence Ca^{2+} dynamics. In the light, the Ca^{2+} concentration in sea water decreases due to Ca^{2+} diffusion for calcification (Borowitzka and Larkum 1976a; De Beer and Larkum 2001). Borowitzka and Larkum (1976b) showed that the rate of calcification is proportional to the photosynthetic rate; for every mole of $CaCO_3$ precipitated, 4–8 mol of CO_2 must be fixed in photosynthesis.

Ocean acidification and ocean warming as drivers of calcification and photosynthesis inhibition in *Halimeda*

Negative calcification rates were observed in *H. macroloba* and *H. cylindracea* under high pCO_2 conditions, independent of treatment temperature, suggesting that dissolution of the calcium carbonate structure occurred primarily in response to shifts in carbonate chemistry, rather than increased temperature. The elevated pCO_2 in the treatments changed the carbonate chemistry of sea water by decreasing the availability of CO_3^{2-} ions required for calcification and resulted in a decreased aragonite saturation state (Ω_a) to 1.97 ± 0.02 and 2.05 ± 0.01 (mean ± SE) at pH 7.7, 28 and 32 °C, respectively (Table 1). This finding is consistent with the previous studies that observed negative calcification rates and decreasing aragonite crystal width in *Halimeda* spp. (Sinutok et al. 2011) under ocean acidification and ocean warming conditions.

Increases in pCO_2 are expected to promote photosynthesis and growth in some marine phototrophs such as seagrasses, and non-calcifying macroalgae, due to an increased availability of inorganic carbon sources for photosynthesis (Gao et al. 1993; Short and Neckles 1999; Palacios and Zimmerman 2007). However, we found that 5 weeks at elevated pCO_2 lead to a decline in Chl *a* and *b* concentration in both temperature treatments, indicating decreased chlorophyll production or pigment degradation in *Halimeda*, leading to less capacity for light absorption and photosynthesis. Reductions in PSII photochemical efficiency (F_V/F_M and $\Delta F/F_M'$) were observed at elevated pCO_2 and temperature treatments, similar to the previous findings (Sinutok et al. 2011) indicating a loss of functional PSII reaction centres, downregulation of photochemistry and/or photoinhibition. In addition, increases in the maximum excitation pressure (Q_m), an indicator of non-photochemical quenching, were observed under elevated pCO_2 and temperature stress. Values close to 1 were observed in the high CO_2 and temperature treatment, indicating that most of the PSII reaction centres are closed under maximum irradiance increasing the potential for photoinhibition (Iglesias-Prieto et al. 2004).

Under ocean acidification and ocean warming conditions, the reductions in PSII photochemical efficiency (F_V/F_M and $\Delta F/F_M'$) and increases in the maximum excitation pressure (Q_m) suggested that the level of non-photochemical quenching was elevated via heat dissipation. Both observations indicated a decrease in physiological performance and the onset of a combination of photoprotective processes and photoinhibition in these species under pH and thermal stress (Iglesias-Prieto et al. 2004; Kuguru et al. 2010). Our results from O_2 microprofiles support the photosynthetic pigment and chlorophyll fluorescence data, showing decreasing O_2 production with declining Chl *a* and *b* concentrations and a decreased photosynthetic efficiency under pH and/or heat stress (Table 2; Figs. 1–6).

Ecological implications

A recent study in a naturally high CO_2 region at volcanic vents off Ischia Island, Italy, observed high seagrass production and a lack of calcifying organisms (e.g. *Halimeda* and corals) at pH 7.6 and $\Omega_a < 2.5$ (Hall-Spencer et al. 2008). Our study is consistent with those findings and indicates that rising pCO_2 and temperature will have a negative impact on photosynthesis and calcification in *Halimeda* leading to a reduction in its abundance and primary productivity on coral reefs. We found strong effects of temperature and pCO_2 on the microenvironment of two *Halimeda* species, as well as significant reductions in physiological performance. As an ecosystem engineer and a key sediment producer, the loss or severe decline of *Halimeda* from reef ecosystems will thus have a dramatic impact on carbonate accumulation, sediment turnover, habitat structure as well as trophic food webs associated with these species.

Acknowledgments We thank Louise Evans and Linda Xiao and the School of Chemistry and Forensic Science, University of Technology, Sydney, for assistance with the autotitrator. Anthony Larkum, Daniel Nielsen, Daniel Wangpraseurt and Ponlachart Chotikarn are thanked for their assistance with microsensor experimental set-ups. This project was supported by the Plant Functional Biology and Climate Change Cluster, School of the Environment, University of Technology, Sydney, an Australian Coral Reef Society student research award (SS), and the Phycological Society of America Grant-in-Aid of Research award (SS). Additional support was due to the Danish Natural Science Research Council (MK). The research was performed under Great Barrier Reef Marine Park Authority permit G09/30853.1.

References

Al-Horani FA (2005) Effects of changing seawater temperature on photosynthesis and calcification in the scleractinian coral

Galaxea fascicularis, measured with O_2, Ca^{2+} and pH microsensors. Sci Mar 69:347–354

Allakhverdiev SI, Kreslavski VD, Klimov VV, Los DA, Carpentier R, Mohanty P (2008) Heat stress: an overview of molecular responses in photosynthesis. Photosynth Res 98:541–550

Anthony KRN, Kline DI, Diaz-Pulido G, Dove S, Hoegh-Guldberg O (2008) Ocean acidification causes bleaching and productivity loss in coral reef builders. Proc Natl Acad Sci USA 105:17442–17446

Baker NR (2008) Chlorophyll fluorescence: a probe of photosynthesis in vivo. Annu Rev Plant Physiol 59:89–113

Blaxter JHS, Russel FS, Young M (eds) (1980) Ecology and taxonomy of *Halimeda*: primary producer of coral reefs. Academic Press, New York

Borowitzka MA (1977) Algal calcification. Oceanogr Mar Biol Annu Rev 15:189–223

Borowitzka MA (1986) Physiology and biochemistry of calcification in the Chlorophyceae. In: Leadbeater B, Riding H (eds) Biomineralization in the lower plants and animals. Oxford University Press, Oxford, pp 107–124

Borowitzka MA (1989) Carbonate calcification in algae—initiation and control. In: Mann S, Webb J, Williams RJP (eds) Biomineralization: Chemical and biochemical perspectives. VCH, Weinheim, pp 63–94

Borowitzka MA, Larkum AWD (1976a) Calcification in the green alga *Halimeda* II. The exchange of Ca^{2+} and the occurrence of age gradients in calcification and photosynthesis. J Exp Bot 27:864–878

Borowitzka MA, Larkum AWD (1976b) Calcification in the green alga *Halimeda* III. The sources of inorganic carbon for photosynthesis and calcification and a model of the mechanism of calcification. J Exp Bot 27:879–893

Borowitzka MA, Larkum AWD (1977) Calcification in the green alga *Halimeda*. I. An ultrastructure study on thallus development. J Phycol 13:6–16

Borowitzka MA, Larkum AWD, Nockolds CE (1974) A scanning electron microscope study of the structure and organization of the calcium carbonate deposits of algae. Phycologia 13:195–203

De Beer D, Larkum AWD (2001) Photosynthesis and calcification in the calcifying algae *Halimeda discoidea* studied with microsensors. Plant, Cell Environ 24:1209–1217

Diaz-Pulido G, McCook LJ, Larkum AWD, Lotze HK, Raven JA, Schaffelke B, Smith JE, Steneck RS (2007) Vulnerability of macroalgae of the Great Barrier Reef to climate change. In: Johnson JE, Marshall PA (eds) Climate change and the Great Barrier Reef. Great Barrier Reef Marine Park Authority and Australian Greenhouse Office, Australia, pp 153–192

Drew EA (1983) *Halimeda* biomass, growth rates and sediment generation on reefs in the Central Great Barrier Reef Province. Coral Reefs 2:101–110

Feely RA, Sabine CL, Lee K, Berelson W, Kleypas J, Fabry VJ, Millero FJ (2004) Impact of anthropogenic CO_2 on the $CaCO_3$ system in the oceans. Science 305:362–366

Fujita K, Hikami M, Suzuki A, Kuroyanagi A, Sakai K, Kawahata H, Nojiri Y (2011) Effects of ocean acidification on calcification of symbiont-bearing reef foraminifers. Biogeosciences 8:2089–2098

Gao K, Aruga Y, Asada K, Kiyohara M (1993) Influence of enhanced CO_2 on growth and photosynthesis of the red algae *Gracilaria* sp. and *G. chilensis*. J Appl Phycol 5:563–571

Gattuso J-P, Lavigne H (2009) Technical note: approaches and software tools to investigate the impact of ocean acidification. Biogeosciences 6:2121–2133

Glud RN, Gundersen JK, Revsbech NP, Jørgensen BB (1995) Effects on the benthic diffusive boundary layer imposed by microelectrodes. Limnol Oceanogr 39:462–467

Guinotte JM, Buddemeier RW, Kleypas JA (2003) Future coral reef habitat marginality: temporal and spatial effects of climate change in the Pacific basin. Coral Reefs 22:551–558

Hall-Spencer JM, Rodolfo-Metalpa R, Martin S, Ransome E, Fine M, Turner SM, Rowley SJ, Tedesco D, Buia M-C (2008) Volcanic carbon dioxide vents show ecosystem effects of ocean acidification. Nature 454:96–99

Hill R, Larkum AWD, Frankart C, Kühl M, Ralph PJ (2004) Loss of functional photosystem II reaction centres in zooxanthellae of corals exposed to bleaching conditions: using fluorescence rise kinetics. Photosynth Res 82:59–72

Hofmann LC, Yildiz G, Hanelt D, Bischof K (2012) Physiological responses of the calcifying rhodophyte, *Corallina officinalis* (L.), to future CO_2 levels. Mar Biol 159:783–792

Houghton J (2009) Global warming: the complete briefing. Cambridge University Press, United Kingdom

Iglesias-Prieto R, Beltrán VH, LaJeunesse TC, Reyes-Bonilla H, Thome PE (2004) Different algal symbionts explain the vertical distribution of dominant reef corals in the eastern Pacific. Proc R Soc Biol Sci Ser B 271:1757–1763

Jokiel PL, Maracios JE, Franzisket L (eds) (1978) Coral growth: buoyant weight technique. In: Stoddart DR, Johannes RE (eds) Coral reefs: Research methods, UNESCO, pp 529–541

Jokiel PL, Rodgers KS, Kuffner IB, Andersson AJ, Cox EF, Mackenzie FT (2008) Ocean acidification and calcifying reef organisms: a mesocosm investigation. Coral Reefs 27:473–483

Kleypas JA, Yates KK (2009) Coral reefs and ocean acidification. Oceanography 22:108–117

Kleypas JA, Buddemeier RW, Archer D, Gattuso J-P, Langdon C, Opdyke BN (1999) Geochemical consequences of increased atmospheric carbon dioxide on coral reefs. Science 284:118–120

Köhler-Rink S, Kühl M (2000) Microsensor studies of photosynthesis and respiration in larger symbiotic foraminifera. I The physio-chemical microenvironment of *Marginopora vertebralis*, *Amphistegina lobifera* and *Amphisorus hemprichii*. Mar Biol 137:473–486

Köhler-Rink S, Kühl M (2005) The chemical microenvironment of the symbiotic planktonic foraminifer *Orbulina universa*. Mar Biol Res 1:68–78

Kuffner IB, Andersson AJ, Jokiel PL, Rodgers KS, Mackenzie FT (2007) Decreased abundance of crustose coralline algae due to ocean acidification. Nat Geosci 1:114–117

Kuguru B, Achituv Y, Gruber DF, Tchernov D (2010) Photoacclimation mechanisms of corallimorpharians on coral reefs: photosynthetic parameters of zooxanthellae and host cellular responses to variation in irradiance. J Exp Mar Biol Ecol 394:53–62

Langdon C, Gattuso J-P, Anderson A (2010) Measurements of calcification and dissolution of benthic organisms and communities. In: Riebesell U, Fabry VJ, Hansson L, Gattuso J-P (eds) Guide to best practices for ocean acidification research and data reporting. Publication Office of the European Union, Luxembourg, pp 213–232

Larkum AWD, Salih A, Kühl M (2011) Rapid mass movement of chloroplasts during segment formation of the calcifying siphonalean green alga *Halimeda macroloba*. PLoS One 6. doi: 10.1371/journal.pone.0020841

Lewis E, Wallace DWR (1998) CO2SYS—Program developed for the CO2 system calculations. Carbon Dioxide Information Analysis Center; Report ORNL/CDIAC-105, Oakridge National Laboratory, Oakridge, TN

Maxwell K, Johnson GN (2000) Chlorophyll fluorescence—a practical guide. J Exp Bot 51:659–668

McConnaughey T (1989) Biomineralization mechanisms. In: Crick RE (ed) Origin, evolution, and modern aspects of biomineralization in plants and animals. Plenum Press, New York, pp 57–73

McConnaughey TA, Whelan JF (1997) Calcification generates protons for nutrient and bicarbonate uptake. Earth-Sci Rev 42:95–117

Palacios SL, Zimmerman RC (2007) Response of eelgrass *Zostera marina* to CO_2 enrichment: possible impacts of climate change

and potential for remediation of coastal habitats. Mar Ecol Prog Ser 344:1–13

Revsbech NP, Jorgensen BB, Brix O (1981) Primary production of microalgae in sediments measured by oxygen microprofile, $H^{14}CO_3^-$ fixation, and oxygen exchange methods. Limnol Oceanogr 26:717–730

Ries JB (2011) A physicochemical framework for interpreting the biological calcification response to CO_2-induced ocean acidification. Geochim Cosmochim Acta 75:4053–4064

Ritchie RJ (2008) Universal chlorophyll equations for estimating chlorophylls *a, b, c*, and *d* and total chlorophylls in natural assemblages of photosynthetic organisms using acetone, methanol, or ethanol solvents. Photosynthetica 46:115–126

Schreiber U (2004) Pulse-amplitude-modulation (PAM) fluorometry and saturation pulse method: An overview. In: Papageorgiou GC, Govindjee (eds) Chlorophyll *a* fluorescence: A signature of photosynthesis. Springer, Dordrecht, pp 279–319

Short FT, Neckles HA (1999) The effects of global climate change on seagrasses. Aquat Bot 63:169–196

Sinutok S, Hill R, Doblin MA, Wuhrer R, Ralph PJ (2011) Warmer more acidic conditions cause decreased productivity and calcification in subtropical coral reef sediment-dwelling calcifiers. Limnol Oceanogr 56:1200–1212

Smith SV, Kinsey DW (1976) Calcium carbonate production, coral reef growth, and sea level change. Science 194:937–939

Warner ME, Fitt WK, Schimidt GW (1999) Damage to photosystem II in symbiotic dinoflagellates: a determinant of coral bleaching. Proc Natl Acad Sci USA 96:8007–8012

Weyl PK (1959) The change in solubility of calcium carbonate with temperature and carbon dioxide content. Geochim Cosmochim Acta 17:214–225